

## Article

# Performance of Anisole and Isobutanol as Gasoline Bio-Blendstocks for Spark Ignition Engines

Michał Wojcieszek <sup>1,\*</sup> , Lotta Knuutila <sup>1</sup> , Yuri Kroyan <sup>1</sup> , Mário de Pinto Balsemão <sup>1</sup> , Rupali Tripathi <sup>2</sup> , Juha Keskiivali <sup>2</sup> , Anna Karvo <sup>2</sup> , Annukka Santasalo-Aarnio <sup>1</sup> , Otto Blomstedt <sup>1</sup> and Martti Larmi <sup>1</sup> 

<sup>1</sup> Department of Mechanical Engineering, School of Engineering, Aalto University, 02150 Espoo, Finland; lotta.knuutila@aalto.fi (L.K.); yuri.kroyan@aalto.fi (Y.K.); majocax@gmail.com (M.d.P.B.); annukka.santasalo@aalto.fi (A.S.-A.); otto.blomstedt@aalto.fi (O.B.); martti.larmi@aalto.fi (M.L.)

<sup>2</sup> Neste Corporation, 02150 Espoo, Finland; rupali.tripathi@neste.com (R.T.); juha.keskiivali@neste.com (J.K.); anna.karvo@neste.com (A.K.)

\* Correspondence: michal.wojcieszek@aalto.fi; Tel.: +358-50-472-3055

**Abstract:** Several countries have set ambitious targets for the transport sector that mandate a gradual increase in advanced biofuel content in the coming years. The current work addresses this transition and indicates two promising gasoline bio-blendstocks: anisole and isobutanol. The whole value chains of these bio-components were considered, focusing on end-use performance, but also analyzing feedstock and its conversion, well-to wheel (WTW) greenhouse gas (GHG) emissions and costs. Three alternative fuels, namely a ternary blend (15% anisole, 15% isobutanol, 70% fossil gasoline on an energy basis) and two binary blends (15% anisole with fossil gasoline and 30% isobutanol with fossil gasoline), were tested, focusing on their drop-in applicability in spark ignition (SI) engines. The formulated liquid fuels performed well and showed the potential to increase brake thermal efficiency (BTE) by 1.4% on average. Measured unburned hydrocarbons (HC) and carbon monoxide (CO) emissions were increased on average by 12–29% and 17–51%, respectively. However, HC and CO concentrations and exhaust temperatures were at acceptable levels for proper catalyst operation. The studied blends were estimated to bring 11–22% of WTW GHG emission reductions compared to base gasoline. Additionally, the fleet performance and benefits of flexi-fuel vehicles (FFV) were modeled for ternary blends.

**Keywords:** anisole; isobutanol; renewable gasoline; fuel blends; spark ignition engine performance; emissions



**Citation:** Wojcieszek, M.; Knuutila, L.; Kroyan, Y.; de Pinto Balsemão, M.; Tripathi, R.; Keskiivali, J.; Karvo, A.; Santasalo-Aarnio, A.; Blomstedt, O.; Larmi, M. Performance of Anisole and Isobutanol as Gasoline Bio-Blendstocks for Spark Ignition Engines. *Sustainability* **2021**, *13*, 8729. <https://doi.org/10.3390/su13168729>

Academic Editors: Luca Marchitto and Cinzia Tornatore

Received: 23 June 2021

Accepted: 25 July 2021

Published: 5 August 2021

**Publisher's Note:** MDPI stays neutral with regard to jurisdictional claims in published maps and institutional affiliations.



**Copyright:** © 2021 by the authors. Licensee MDPI, Basel, Switzerland. This article is an open access article distributed under the terms and conditions of the Creative Commons Attribution (CC BY) license (<https://creativecommons.org/licenses/by/4.0/>).

## 1. Introduction

Transportation is a hard-to-abate sector that emitted roughly a quarter of global energy-related carbon dioxide (CO<sub>2</sub>) emissions in 2019 [1]. On the European Union (EU) level, it accounted for 32% of EU-28 GHG emissions in 2017, while passenger cars were responsible for around 44% of transport emissions [2]. The light-duty vehicle (LDV) fleet in the EU is growing and cars fueled with gasoline or diesel cover over 95% of the market [3]. Moreover, the new sales are dominated (over 60% in EU) by powertrains equipped with spark ignition engines using gasoline [4]. Consequently, currently sold vehicles [5,6] will make up an average fleet in 2030 and beyond, meaning that gasoline-fueled engines will still be highly represented on roads within the coming decades. Therefore, it is evident that renewable gasoline bio-blendstocks will be needed to meet ambitious energy and climate targets. In the EU, provisions for the year 2030 are included in National Energy and Climate Plans [7]. In Finland, for instance, the renewable energy in transport should reach 30% by 2030 [8], with a separate 10% sub-target for advanced biofuels [9]. The advanced biofuels are defined by a recast of the Renewable Energy Directive (RED II), while Part A of Annex IX lists suitable types of feedstock which can bring substantial GHG emissions savings [10]. On the other hand, in RED II, a great deal of attention has been paid to electric

vehicles (EV), which are seen as a promising solution for the LDV sector [11]. However, the complete electrification of the passenger car fleet is not an immediate process [12] and will require a great deal of resources [13]. It needs to be complemented by other solutions, preferably compatible with the current infrastructure [14], to meet GHG reduction goals. Hence, sustainable bio-derived drop-in fuel components are appealing options that could help to decarbonize the transport sector in the mid-term perspective.

This work addresses challenges related to the decarbonization of light-duty road transport. Even though there is a solution for replacing fossil diesel by using renewable high-quality diesel [15], gasoline-like drop-in fuels with high bio-content are still under development. Hence, this study examines anisole and isobutanol as chemicals exhibiting the potential to be direct bio-blendstocks for gasoline fuel used in spark ignition engines. The present knowledge about the SI engine performance of anisole and isobutanol fuels is limited to a few demonstrations of low/medium-concentration blends of isobutanol or low-concentration anisole binary blends. This study investigates medium-concentration blends of anisole and isobutanol. The experimental part focuses on tests of three selected blends, including a ternary blend, in the SI engine of a regular LDV, over steady-state conditions. The modeling part extends the scope to the variable composition of ternary blends, where the end-use performance is simulated over the whole fleet of FFV.

## 2. Research Background

### 2.1. Biocomponents in Gasoline

Gasoline, as a balanced mixture of multiple components, offers an opportunity to blend new chemical compounds stemming from renewable feedstock instead of crude oil. In the Co-Optima initiative, which focuses on the simultaneous co-optimization of fuels and engines, the top blendstocks for turbocharged spark ignition engines were identified [16,17]. Various alcohols and other chemical groups, such as olefins, furans, and ketones, were examined, whereas the screening was done by assessing critical fuel properties [18]. The initiative resulted in the merit function indicating bio-blendstocks with the potential to enhance the performance of modern SI engines [19,20]. Another study was conducted at Aachen University, where the multiproduct biorefinery concept was developed based on supply chain and final product selection [21]. In this research, biofuel blends were formulated by the model, which simultaneously took into account fuel product and conversion pathway design [22]. The formulated fuel blends were evaluated according to the production cost and global warming impact [23]. The study proposed tailor-made fuels containing isobutanol, among a few other compounds [24].

In this study, anisole and isobutanol were selected as potential blending candidates by considering the entire value chain. This includes sustainable feedstock and its conversion methods, engine compatibility, end-use performance, GHG emission reduction potential, and estimated price. Important raw materials for the production of both selected compounds could be forest residues [25], lignin [26], agricultural waste [27], and lignocellulosic herbaceous biomass [28]. The use of these feedstock types in biochemical and thermochemical conversion processes offers substantial WTW GHG savings compared to fossil gasoline [29]. Additionally, anisole and isobutanol exhibit favorable end-use properties and could be used in optimized SI engines in the LDV sector [30].

### 2.2. Anisole

Anisole is an aromatic ether which consists of an aromatic ring and a methoxy-group. Renewable anisole can be found in bio-oil from fast pyrolysis [31] or biocrude from hydrothermal liquefaction (HTL) [32]. Both pyrolysis and HTL are thermochemical processes of biomass conversion into liquids. Low-moisture-content feedstock can be used for the production of bio-oil [33]. As an example, residual lignin from the pulping process is seen as a viable raw material [34]. Furthermore, wet feedstock can be subject to the HTL process, whereas the resulting biocrude can be further upgraded into drop-in biofuel [35].

Anisole has favorable properties to become a gasoline bio-blendstock. It improves the stability and storability of gasoline, unlike other promising components, such as alkylated furans [36]. Gschwend et al. [37] concluded that anisole is no more toxic than base gasoline. In the same study, modeling results showed a decrease in volumetric fuel consumption for neat anisole, whereas CO<sub>2</sub> and particulate emissions increased compared to fossil gasoline. McCormick et al. [18] mentioned the positive effect of anisole blending on research octane number (RON) but also reported a negative effect on the distillation curve, especially the 50% evaporation temperature (T<sub>50</sub>), for blends with gasoline. Anisole is seen as a promising SI fuel component primarily due to its high RON [38] and octane sensitivity [39], low reactivity [40], and high laminar flame speed [41]. Despite this, few engine tests with anisole blends have been reported in the literature so far. Tian et al. [39] concentrated on the anti-knock quality of lignin-derived compounds. Among various aromatic oxygenates, a 10% volumetric blend of anisole with gasoline was also tested on a boosted LDV SI engine with port fuel injection (PFI). The addition of anisole increased the octane number of the fuel and, because of this, it was possible to operate the engine with an earlier knock-limited spark advance. In another study, Szybist et al. [42] tested an anisole blend in a single-cylinder SI engine with a direct injection (DI) system. The authors investigated a 25% molar blend of anisole with gasoline in the context of the knock effect and highlighted that the anisole blend consistently overperformed based on its expected knock propensity. In another experimental study, Ratcliff et al. [43] tested a 20% volumetric blend of anisole with gasoline in a DI single-cylinder LDV engine, where RON was an adequate measure to predict the knock-limited performance.

### 2.3. Isobutanol

Isobutanol, an isomer of butanol, is a branched four-carbon alcohol with a hydroxyl group attached to the first carbon atom. It can be produced from fossil resources but also from biomass, often sharing feedstocks with ethanol [44]. Renewable isobutanol is obtained in a biochemical conversion process, in which sugars originating from corn, sugar cane, or wheat are subjected to fermentation [45]. The production of isobutanol starting from herbaceous biomass has also been demonstrated [30,45]. Other lignocellulosic feedstocks (i.e., corn stover), after a suitable pretreatment, can be subjected to a fermentation process, performed by genetically engineered microorganisms such as *Escherichia coli* and *Saccharomyces cerevisiae* strains [27]. Isobutanol is toxic for the microorganisms and it limits the sugar concentration in the fermentation broth [46]. Therefore, Roussos et al. [27] suggested integrated isobutanol removal in the fermentation stage to ensure the proper functioning of microorganisms. Baez et al. [47] have shown a similar solution and applied gas stripping to separate the product and lower the energy consumption. In another example, Gevo Integrated Fermentation Technology was used to continuously remove the product during the fermentation process [48].

Isobutanol, compared to other alcohols such as ethanol or methanol, has the closest lower heating value (LHV) to gasoline [37]. It is recognized as a good gasoline blending component due to its high RON and lower solubility in water [29]. This, in turn, allows the use of isobutanol in unmodified SI engines in higher concentrations than ethanol [49,50]. The EN228 standard for gasoline allows a maximum 15% volume-based content of isobutanol in the fuel blend with commercial gasoline. Among isomers of butanol, isobutanol has the highest RON of 105.5 and a synergistic blending effect with base gasoline [16]. Isobutanol has much lower Reid Vapor Pressure than gasoline (approximately 3.1 kPa at 37.8 °C [51]) along with a significantly higher heat of vaporization (508 kJ/kg), and roughly 20% lower LHV [16]. In the Co-Optima study, McCormick et al. [18] highlighted isobutanol as one of the most promising biomass-derived SI fuel compounds. Moreover, isobutanol performs well in SI engines. According to the studies by Stansfield et al. [52] on a regular passenger car SI engine, 16% and 68% blends of isobutanol increase the volumetric fuel consumption by 2% and 12%, respectively. On the other hand, both blends bring reductions in tailpipe CO<sub>2</sub> emissions, by 0.18–1.05% compared to base gasoline.

Isobutanol, as well as other alcohols, performs much better in the fleet of flexible fuel vehicles. Karavalakis et al. [53] tested a 55% isobutanol blend in an FFV and the results showed slightly higher volumetric fuel consumption of 1.7% and nearly 4% lower tailpipe CO<sub>2</sub> emissions compared to gasoline.

#### 2.4. Merits of FFV

The optimization of internal combustion engines (ICE) is gaining higher importance when thinking about premium biofuels. A good justification for this statement could be found for fuels that have RON beyond 95 (base gasoline). Higher RON means that fuel can resist auto-ignition at higher compression ratios (CR) [54]. In this case, applying higher CR results in a better thermal efficiency of the ICE [55]. The CR could be increased via geometric configuration or by changing the effective compression ratio via advanced ignition timing, boosting the intake pressure, and variable valve timing [56]. Vehicles equipped with flexible-fuel engines allow them to operate with high-concentration alcohol fuels such as E85 but also with regular gasoline. FFVs have fuel feedback control systems that adjust fuel delivery and ignition timing according to the given fuel that the engine is operating with [57]. This allows FFVs to operate more efficiently with fuels of good anti-knocking characteristics (including bio-butanol [58]) compared to regular SI engines, and thus improve the fuel economy.

### 3. Materials and Methods

This paper provides a complete assessment of anisole and isobutanol, the selected SI fuel blending components, looking at their whole value chains, with the main focus on end-use performance. The consecutive steps of this research, together with the resulting key outcomes, are presented in Figure 1. In the first step, anisole and isobutanol were considered based on the available literature. The study focused on feedstock, production pathways, and compatibility with SI engines. In the next step, four selected fuels were experimentally tested on an SI engine and the results analyzed in the context of efficiency and emissions. Additionally, the end-use performance of ternary blends was modeled for FFVs. In the final step, the tested fuels were assessed from an environmental perspective, focusing on GHG emissions and costs.

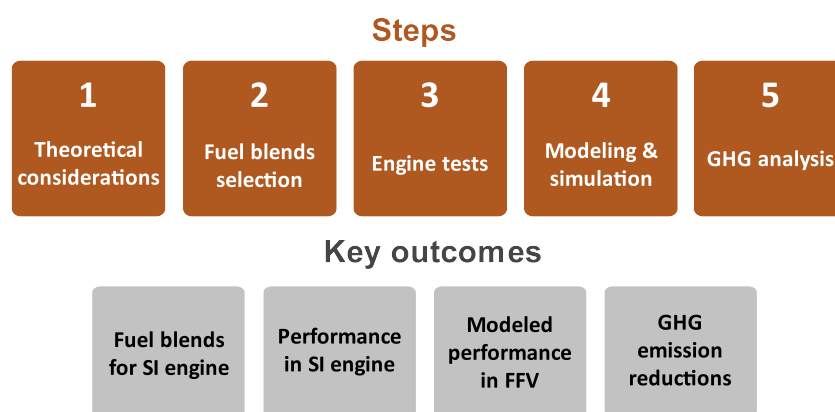


**Figure 1.** Consecutive steps and key outcomes resulting from this study.

#### 3.1. Tested Fuels

Four fuels, prepared for experimental tests, are described in Table 1. The anisole binary blend meets the oxygen limits of the EN228 standard, whereas the isobutanol binary and ternary blends address the 30% energy content target for biofuels. Base gasoline was blended for research purposes by Neste. Neat anisole with 99% purity and neat isobutanol also with 99% purity were provided by Thermo Fisher Scientific. The blending was done with the use of volumetric and beaker glasses, fuel pump, and scale. Obtained fuels were stored in canisters in cold conditions (5 °C) before the engine tests.

**Table 1.** Specification of experimentally tested fuels.

		Base Gasoline	Anisole	Isobutanol	Anisole Binary Blend	Isobutanol Binary Blend	Ternary Blend
Energy content [%]	Gasoline	100	0	0	85	70	70
	Anisole	0	100	0	15	0	15
	Isobutanol	0	0	100	0	30	15
RON		95	103	105	96.4	99.2	98.5
LHV <sub>mass</sub> [MJ/kg]		43.6	32.7	33.4	41.5	39.9	39.8
LHV <sub>vol</sub> [MJ/L]		32.6	32.4	26.8	32.5	30.5	31.5
Density [kg/m <sup>3</sup> ]		747	990	802	784	764	791
Molecular Weight [g/mol]		95.9	108.1	74.1	98	86.8	92.9
Oxygen [wt. %]		0.1	14.8	21.6	2.9	7.8	6.6

For each blend presented in Table 1, GHG emissions based on the conversion pathways were calculated. For anisole, the emission factor of 27.2 g CO<sub>2</sub>-eq/MJ from the study by Tews et al. [25] was selected, representing the hydrothermal liquefaction of forest residues. For isobutanol, the emission factor of 25.9 g CO<sub>2</sub>-eq/MJ is based on a study by Cai et al. [30] and it includes lignocellulosic biomass supply chain, biorefinery operations, and combustion. For the base gasoline, the emission factor of 93.3 g CO<sub>2</sub>-eq/MJ was used according to the European Commission [59]. Additionally, the prices of anisole and isobutanol originating from emerging conversion pathways were compared based on literature sources.

### 3.2. Experimental Engine Set-Up and Measurements

The experimental tests of selected fuels were performed on a spark ignition engine—Volvo B4204—with specifications shown in Table 2. This 4-cylinder 2.0-liter engine with a compression ratio of 10.2:1 was turbocharged and equipped with a port fuel injection system.

**Table 2.** Specifications of the engine used in the study.

<b>Engine</b>	Volvo B4204
<b>Engine type</b>	4 cylinders, 4 valves per cylinder
<b>Displacement volume</b>	1.95 dm <sup>3</sup>
<b>Bore × stroke</b>	83 × 90 mm
<b>Compression ratio</b>	10.2:1
<b>Power</b>	120 kW
<b>Injection system</b>	Port fuel injection (PFI)
<b>Charge cooling</b>	Air-cooled
<b>Boosting system</b>	Turbocharger Garret Gt3071
<b>EGR</b>	No

The engine on the test bench was coupled to the Schenk W260 eddy-current dynamometer. The engine control unit (ECU) used was Vipec V88, and all of the sensors were connected to the computer and parameters were monitored via LabView software. The schematic of the experimental test bed is presented in Figure 2. The test strategy was to apply stoichiometric combustion, while lambda was controlled by the engine sensor. The main focus of blend testing was to check drop-in applicability in engines optimized for base gasoline. Therefore, the spark timing was chosen for the highest torque in the base gasoline case and, afterward, it was treated as a fixed parameter. Engine operation was performed

at six steady-state points with various engine speeds and loads. The selected steady-state points try to mimic the real driving conditions in urban and also highway conditions for Volvo S40 at a constant speed in the selected gear (engine operating conditions including engine speed and load, are calculated based on the vehicle speed, tire radius, gear ratio, and total running resistance of the car, following guidelines in [60]). Therefore, the load sweep represents actual engine operating conditions for regular use in the passenger car. Each selected steady-state operation can be associated with specified brake mean effective pressure (BMEP) in range 1.5–4.6 bars—see Table 3.

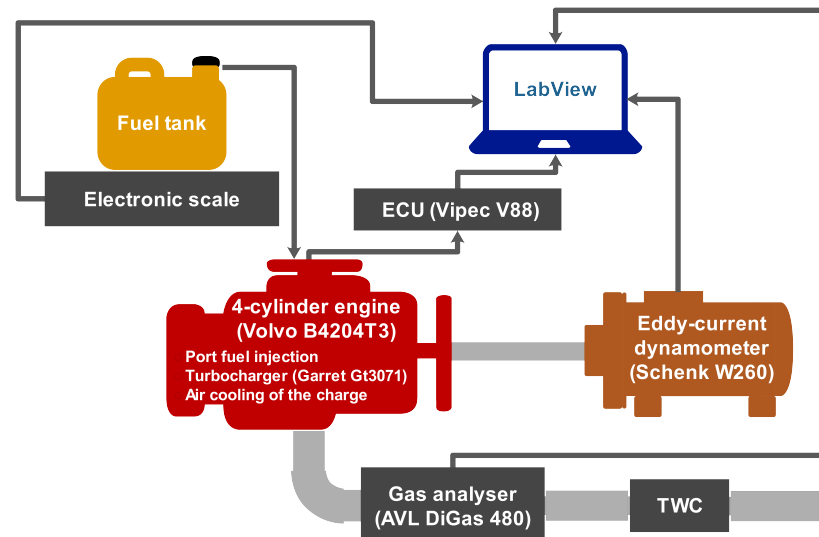


Figure 2. Schematic diagram of the engine test bed.

Table 3. Engine operating conditions for selected test points.

Steady State	Engine Speed [rpm]	Load [Nm]	Load [% of max]	BMEP [bar]	Corresponding Vehicle Speed and Gear Number
1	1550	23	10	1.5	50 km/h, 4th
2	1470	33	14	2.1	60 km/h, 5th
3	1700	38	16	2.4	70 km/h, 5th
4	2000	43	18	2.7	80 km/h, 5th
5	2500	54	23	3.5	100 km/h, 5th
6	3000	70	29	4.6	120 km/h, 5th

All the test results were averaged over time. For the emissions monitoring (HC, CO), AVL DiGas 480 sensor (AVL 1000) was used. Emissions were measured before three-way catalyst (TWC). No PM emissions were monitored as the engine was equipped with a PFI system and increased PM emissions are rather expected for direct injection systems [61]. The fuel flow was obtained from the electronic scale. Moreover, the exhaust manifold temperature was monitored. The CO<sub>2</sub> emissions were calculated based on the fuel consumption and carbon balance method.

### 3.3. Modeling Performance of Ternary Blends in FFV

In this section, the end-use performance of ternary blends was simulated for flexi-fuel vehicles. Ternary blends composed of base gasoline, anisole, and isobutanol with a volumetric concentration of renewable compounds up to 40% were analyzed. The modeling methodology demonstrated by Kroyan et al. [62] showed that fuel consumption over the driving cycle could be simulated with high accuracy, using a significant set of fuel properties. Properties of ternary blends were estimated based on the interpolation of values related to neat components characterized in Table 4. All properties were interpolated linearly and volumetric LHV and density were calculated using the volumetric composition

of blends. The mass-based LHV and concentrations of hydrogen, carbon, and oxygen were calculated based on the mass composition of the blends. The RON, motor octane number (MON) values, and average molecular weights were estimated based on the molar contribution of the blending components [63].

**Table 4.** Summary of properties for neat gasoline, isobutanol, and anisole used in modeling procedure ('S'—octane sensitivity, 'AMW'—average molecular weight).

Fuel	RON	MON	S	LHV <sub>vol</sub> MJ/L	LHV <sub>mass</sub> MJ/kg	Density g/L	O % wt.	C % wt.	H % wt.	AMW g/mol
Gasoline	95.0	84.8	10.2	32.6	43.6	747.3	0.1	86.4	13.6	95.9
Isobutanol	105.0	90.0	15.0	26.8	33.4	802.0	21.6	64.8	13.6	74.1
Anisole	103.0	91.0	12.0	32.4	32.7	990.0	14.8	77.7	7.5	108.1

The FFV model selected for engine performance analysis (Wojcieszek et al. [64]) was developed based on experimental data coming from both NEDC and FTP test cycles for light-duty vehicles. The model takes RON ( $A$ ), density ( $B$ ), and volume-based LHV ( $D$ ) for estimation of fuel consumption ( $\alpha$ )—see Equation (1). All parameters ( $\alpha$ ,  $A$ ,  $B$ ,  $D$ ) are taken as changes relative to the standard EN228 gasoline.

$$\alpha = -0.418 \cdot A - 1.223 \cdot B - 1.674 \cdot D \quad (1)$$

The CO<sub>2</sub> emissions ( $\beta$ ) were calculated based on the carbon balance using modeled volumetric fuel consumption ( $\alpha$ ), the carbon content of the fuel ( $C$ ), and fuel density ( $\rho$ ), according to Equation (2), where  $\frac{44.01}{12.0107}$  is a molar mass ratio between CO<sub>2</sub> and carbon.

$$\beta \left[ \frac{\text{g}}{\text{km}} \right] = \alpha \left[ \frac{\text{L}}{\text{km}} \right] \cdot \rho \left[ \frac{\text{g}}{\text{L}} \right] \cdot C [\% \text{wt.}] \cdot \frac{44.01}{12.0107} \quad (2)$$

## 4. Results and Discussion

### 4.1. Lignocellulosic Biomass as a Precursor of SI Fuel Component

Lignocellulosic biomass, composed of cellulose, hemicellulose, and lignin, can be used to produce alcohols but also other organic compounds and gasoline-like fuels [65]. The chemical composition of forest or agriculture residues, and their physical properties such as moisture, ash, and inorganic content, are non-negligible parameters in biofuel production [66]. These variables increase the difficulty of utilizing all fractions of lignocellulosic biomass in a single conversion process. In Figure 3, a unique value chain is illustrated as a preliminary concept for a biorefinery design tailored to produce renewable gasoline components from each biomass fraction. Therefore, an integrated and flexible route for both anisole and isobutanol, as well as gasoline-like fuels, offers an interesting and novel approach to biofuel production.

Isobutanol production starting from lignocellulosic biomass is typically carried out via a biochemical conversion route involving fermentation [29]. Biochemical routes based on sugars exhibit lower yields when compared to thermochemical processes due to the inability of utilizing the lignin fraction of lignocellulosic biomass [28]. Therefore, the integration of thermochemical and biochemical conversion routes allows better yields of biofuel production by the simultaneous use of cellulose, hemicellulose, and lignin. This hybrid conversion route, presented in Figure 3, could be optimized for different types of feedstock depending on availability and costs while producing both isobutanol and anisole, as well as a gasoline-like fuel derived from hydrothermal liquefaction or fast pyrolysis processes followed by appropriate catalytic upgrading [67,68]. The production of isobutanol via fermentation [30,48], bio-oil from fast pyrolysis [33,69], and biocrude from HTL [70,71] has already been demonstrated. However, the extraction of anisole from both bio-oil and biocrude is not proven yet. Nevertheless, anisole, due to its molecular structure, can represent phenolic groups commonly found in pyrolysis oil [72]

and is frequently used as a bio-oil surrogate [73,74]. Anisole can be considered a direct gasoline bio-blendstock [39,42,43] or a precursor for further upgrading to gasoline-like products [26,75–78].

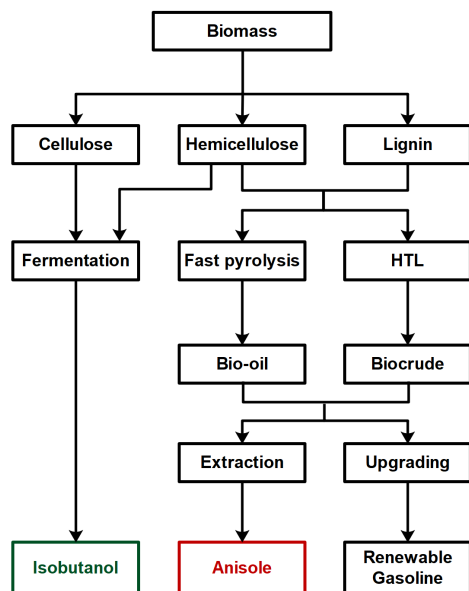


**Figure 3.** Conversion pathways of lignocellulosic biomass to renewable bio-blendstock components, including isobutanol and anisole.

#### 4.2. Experimental Results

All three fuel components (base gasoline, anisole, isobutanol) were completely miscible and no phase separation was observed in the analyzed blends in the concentration range studied. Moreover, no deposits or solid precipitates were found in the samples. The color of the isobutanol binary blend under cold storage conditions changed to orange. This behavior could be explained by a thermochromic phenomenon, which is a reversible change in the color and occurs when the compound is heated or cooled [79]. After one day at room temperature, the sample reverted to a normal yellow color. Additionally, no material compatibility issues were detected for the tested fuel blends. This is in conformity with the literature studies which revealed that higher (55%) isobutanol binary blends exhibit similar material compatibility to E10 gasoline [80]. Although the 15% anisole binary blend did not show any material compatibility issues during the study, it is expected that such issues may arise at higher concentrations, as observed for other oxygenated bio-blendstocks [81].

The results of local emissions measurements (HC, CO) from the PFI spark ignition engine are presented in Figure 4a,b. The trend shows that the higher the engine load, the lower the emissions of unburned hydrocarbons and carbon monoxide. In the case of fuel blends containing oxygenated compounds, local emissions measured without TWC turned out to be elevated. The isobutanol binary blend exhibits the highest HC emissions, especially under lower engine load conditions (Figure 4a). For 1.5 bar engine load, the concentration of HC in exhaust gases reached almost 130 ppm for the isobutanol binary blend, compared to 90 ppm for base gasoline. All tested blends have increased emissions of HC under engine loads between 1.5 and 2.7 bar, while they perform similarly to base gasoline at the highest engine load (4.6 bar), with an HC emission value of 50 ppm. Moreover, there is potential for the anisole blend to slightly decrease HC emissions at higher engine loads. The CO emissions, as in the case of HC, were lowest for the base gasoline (Figure 4b). Again, the largest differences in CO emissions were visible under low-load engine conditions. The ternary blend was characterized by the highest CO emissions, regardless of the engine operating conditions, and the volumetric concentration of CO in exhaust gases exceeded 2% for BMEP in the range 1.5–2.7 bar, whereas the corresponding emissions of base gasoline were around 1.5%. Only at the highest engine load (4.6 bar)

were the CO emissions of all studied fuels on the same level (around 1% concentration in the exhaust).

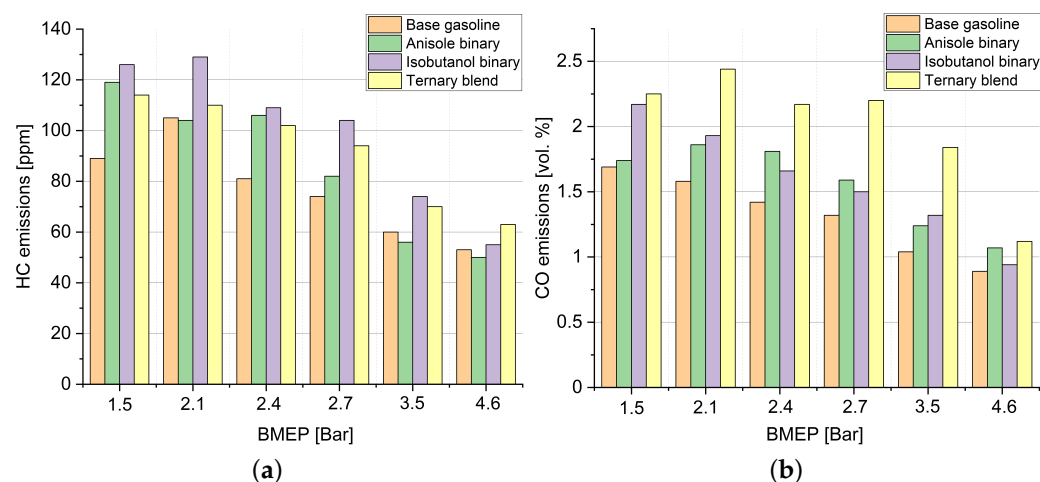
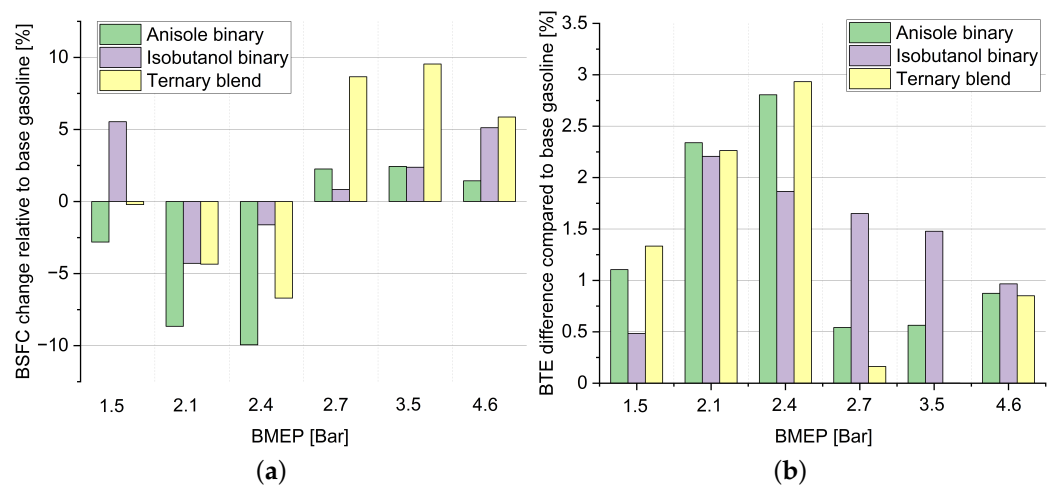


Figure 4. (a) The measured HC and (b) CO emissions before TWC for studied fuels.

Measured CO and HC emissions are bringing new insights into anisole blends' performance in SI engines with the PFI system. In general, the addition of anisole leads to an acceptable increase in both CO and HC emissions. The increase in HC could be attributed to the lower vapor pressure [82] and higher molecular weight of anisole, while the lower H/C ratio could lead to higher CO emissions [83]. The changes for the ternary blend are more visible, especially for CO emissions. However, one could expect a decrease in HC emissions with an increase in isobutanol concentration due to the presence of an oxygen atom in the alcohol molecule [84]. In the current study, only for the highest engine load were the HC and CO emissions very close for the isobutanol binary blend and base gasoline. Such an increase might be caused by significant difference in fuel properties, mainly the higher heat of evaporation and lower vapor pressure of isobutanol, especially at lower engine load/speed conditions [85]. In multiple studies focused on alcohol blends used in SI engines, lower HC and CO emissions were reported [86,87]. However, those results are highly dependent on the experimental set-up and operating conditions. In many cases, full-open throttle engine tests were conducted, which was not the case in the current study. For instance, Elfakhany [88] reported slightly higher CO and HC emissions for two steady states and the opposite trend for another steady-state test condition. In driving cycle test procedures, no definitive trends in HC or CO emissions were observed for increased alcohol content in the blends [89]. When looking at engine set-ups similar to the present study with the PFI injection system, Regalbuto et al. [90] demonstrated differences in the emissions of butanol isomers, with the lowest HC emissions for a 30% isobutanol binary blend at higher engine loads. However, the authors noted a higher concentration of CO in the exhaust gases being over 2% for the isobutanol blend. In another study, Nithyanandan et al. [91] reported an increase in HC emissions while testing 20 and 40% alcohol blends including butanol but observed a drop in CO emissions. Dernote et al. [92] presented a significant increase in CO emissions when operating an engine with slightly richer conditions and a higher concentration of an n-butanol blend. This phenomenon, besides fuel properties (oxygen content, chemical structure, vapor pressure), might be one of the main reasons behind the increase in local emissions.

The results of brake specific fuel consumption (BSFC) and brake thermal efficiency (BTE) are presented in Figure 5a,b. The BSFC decreases with higher engine loads, representing driving at higher vehicle speeds (from 606 g/kWh at 1.5 bar to 338 g/kWh at 4.6 bar for base gasoline). The ternary blend has the highest BSFC at higher engine loads and the increase is around 5–10% compared to base gasoline (Figure 5a). The anisole binary blend performs well in the context of fuel savings, especially for lower engine loads—for

BMEP of 2.4 bar, up to a 10% decrease in BSFC compared to base gasoline is observed. On average, the BSFC decreased by 3.2% in the case of anisole blend while it increased by 1.2% for the two other blends containing isobutanol. From the end-user perspective, the volumetric fuel consumption was observed to slightly decrease for anisole binary (1.8%) and ternary (1.4%) blends, while it increased, on average, by 4.6% for the isobutanol binary blend. These trends are in-line with the previous simulations by Geschwend et al. [37]. The changes in BSFC compared to base gasoline could be explained by differences in LHV. However, all studied blends overperformed based on LHV prediction, which could be attributed to other important fuel properties such as oxygen content, RON, and density, as demonstrated in a previous study [62]. When looking at engine efficiency, the BTE increased from 13.6% up to 24.4% while shifting the engine operation from low to high loads for base gasoline. An improvement in BTE—on average, of 1.4%—was observed for all studied fuel blends when compared with base gasoline (Figure 5b). At the highest engine load, the increase in BTE was 1% for all studied blends, whereas the highest BTE gains (over 2%) were observed at 2.1 and 2.4 bars of BMEP. The current results are in line with other experimental data from the literature. In many studies, the addition of alcohol components positively affects BTE, but leads to an increase in BSFC [86,87,91,93]. For a 10% volumetric blend of anisole, Tian et al. [39] obtained a modest decrease (around 1.5%) in volumetric fuel consumption and no significant changes in BTE. The higher BTE for the studied blends can be attributed to other important fuel properties, mainly higher oxygen content, RON, and heat of evaporation [87]. The engine optimization for higher RON fuels (>95), based on adjusting the spark timing [39,94] or increasing the compression ratio [95], could bring further reductions in BSFC as well as in HC and CO emissions and, in turn, an increase in BTE and lower CO<sub>2</sub> emissions.



**Figure 5.** (a) Changes in BSFC and (b) in BTE for studied fuel blends.

The CO<sub>2</sub> tailpipe emissions for the studied fuel blends, presented in Figure 6a, were calculated based on BSFC and carbon balance. The lowest CO<sub>2</sub> values were found for the isobutanol binary blend in the whole spectrum of engine operating conditions and an average reduction of 7.9% has been achieved. This significant drop is a direct consequence of the lower carbon content compared to base gasoline. The anisole binary and ternary blends also decreased tailpipe CO<sub>2</sub> emissions—both, on average, by 5.1%—compared to base gasoline, mainly due to the decrease in BSFC.

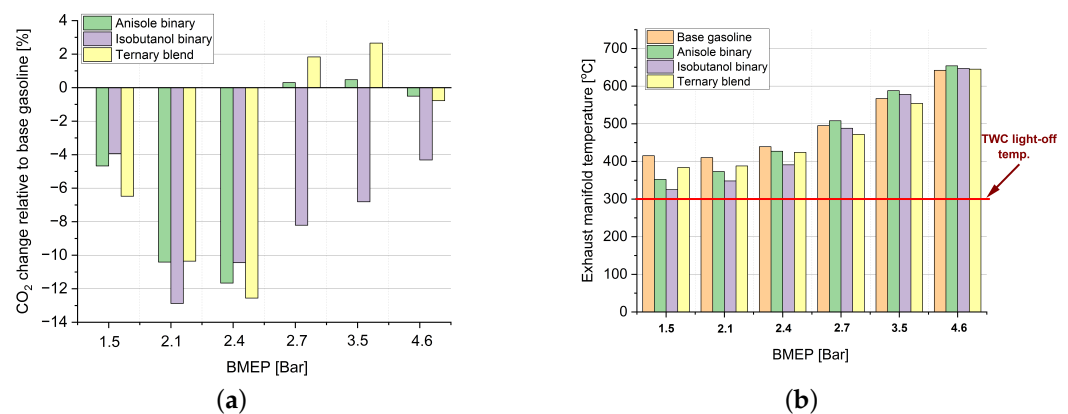


**Figure 6.** (a) Changes in tailpipe CO<sub>2</sub> emissions for studied fuel blends compared to base gasoline. (b) Exhaust temperature after turbine for all tested fuels (catalyst light-off temperature set as 300 °C).

Additionally, the temperature of the exhausts after turbine was measured for the studied blends and compared with base gasoline—see Figure 6b. The results were checked against the catalyst light-off temperature. The operation of TWC needs elevated temperatures above 300 °C [96]. All fuels in the full spectrum of operating conditions fulfilled this requirement. The isobutanol blend exhibited the lowest temperature after turbine, especially at the lowest engine load (325 °C), but still above the TWC light-off limit. The lower exhaust temperature for alcohol blends was also found in other studies [87,91]. Besides exhaust temperature, the HC and CO emission levels were also recognized to be within the acceptable range for proper catalyst operation for all studied blends.

#### 4.3. Modeling Results for the FFV Fleet

This part focuses on the end-use performance of anisole–isobutanol–gasoline ternary blends in the fleet of FFVs via modeling. The end-use performance of ternary blends over the fleet of FFVs was analyzed in terms of volumetric fuel consumption (FC) and carbon dioxide emissions, in both cases relative to base gasoline, which is presented in Figure 7. The FFV modeling results indicate that blends with a high concentration of anisole show a strong reduction in volumetric FC. Moreover, the CO<sub>2</sub> emissions of anisole blends are lower compared to gasoline. Due to the low LHV volume-based of isobutanol, its high-concentration blends represent the highest FC among analyzed ternary blends. However, due to the lowest carbon content, high-concentration isobutanol blends have lower CO<sub>2</sub> emissions compared to base gasoline.

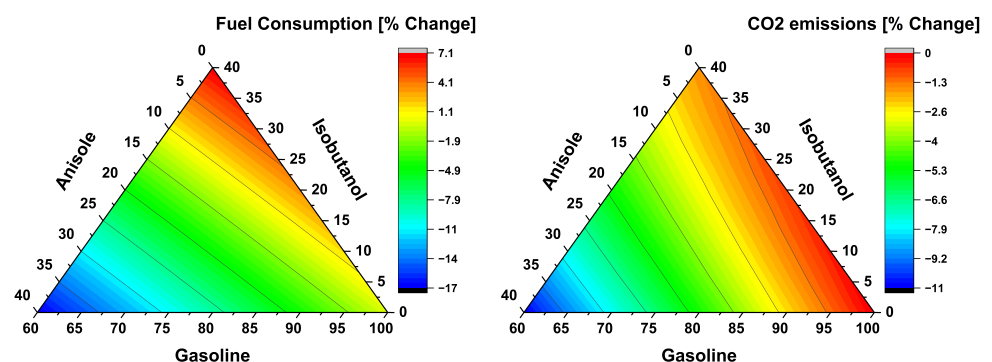


**Figure 7.** Modeled fuel consumption and CO<sub>2</sub> emission changes for FFV fleet for ternary blends in comparison to base gasoline (based on volumetric composition).

The results presented in Figure 7 are in line with the experimental analysis presented in the previous section. The modeled volumetric FC increases by 6.2%, whereas the

increase in average volumetric FC from all steady states equals 4.6% for the isobutanol binary blend. The decrease of 6.1% and 4.1% is modeled for anisole binary and ternary blends, respectively. In comparison to experimental results, the average volumetric FC from all steady states for anisole binary and ternary blends decreases by 1.8% and 1.4%, respectively. Blends of gasoline with anisole and isobutanol have higher RON, which means that they can better resist knocking combustion than base gasoline itself, and this translates to better engine efficiency if the combustion system is optimized. Therefore, one could explain the better performance in the modeled cases compared to the experimental results. Nevertheless, the modeling results refer to driving cycle simulations that include transient operating conditions. It is also important to compare the modeling results with engine or vehicle tests published in the literature. The FFV model shows 4.9% and 7.1% higher FC for the 21% and 55% volumetric binary blends of isobutanol, respectively. The external experimental data for the 55% volumetric binary blend of isobutanol represent an increase of 5.4% in volumetric FC compared to base gasoline [53]. On the other hand, a 21% isobutanol binary blend tested by Aakko-Saksa et al. [49] shows an increase of 0.9% in volumetric FC. The results might differ slightly due to variations in base gasoline properties and the type of engine (size, power, fuel injection strategy, etc.), but, overall, one can conclude that the modeling prediction preserves the experimental result trends for isobutanol binary blends. However, there are no data publicly available on anisole tests in FFV engines for comparison with modeling results.

#### 4.4. GHG Emission Reductions and Cost Estimation

##### 4.4.1. Anisole, HTL Biocrude, and Pyrolysis Bio-Oil

Reductions in GHG emissions could be achieved by fast pyrolysis and hydrothermal liquefaction with the use of lignocellulosic biomass. Anisole can be found in products of both thermochemical processes; however, its extraction has not been proven yet. Therefore, upgraded biocrude and bio-oil are investigated, instead. Table 5 summarizes the available literature knowledge on GHG emission reductions for gasoline-like products from HTL and pyrolysis. It can be concluded that the HTL process could bring higher GHG emission reductions than fast pyrolysis. HTL biocrude could reduce WTW GHG emissions by 71–82%, while fast pyrolysis bio-oil could reduce them by 55–72%, as compared to fossil gasoline.

**Table 5.** Comparison of WTW GHG emissions for fast pyrolysis and HTL processes to obtain gasoline-like products including anisole.

Conversion Process	Feedstock	GHG Emissions [g CO <sub>2</sub> -eq/MJ]	Reference
Fast pyrolysis with upgrading of bio-oil	Logging residues and forest thinnings	33.8	Tews et al. [25]
	Strand board	26.1	
	Corn stover	29.9	
	Clean pine	42.4	Meyer et al. [97]
	Switchgrass	36.9	
Hydrothermal liquefaction process with upgrading to HTL gasoline	Forest residues (small branches)	27.2	Tews et al. [25]
	Forest residues	17–20.5	Nie et al. [98]

The prices of upgraded HTL biocrude and fast pyrolysis bio-oil can be compared. Cai et al. [30] reported that the production of aromatic-rich hydrocarbons via the thermochemical conversion of lignocellulosic biomass would result in a minimum fuel selling price (MFSP) of 1.16 €/L. The MFSP of upgraded HTL bio-crude from forest residues, according

to a study by Tews et al., [25] turned out to be approximately 0.45 €/L. Zhu et al. [99] reached the price of 1.10 €/L for the upgraded HTL biocrude based on a state-of-the-technology case including the HTL process, hydrotreating, and the production of hydrogen. For upgraded fast pyrolysis bio-oil, Tews et al. [25] obtained a price of 0.69 €/L. The upgrading process is more expensive for pyrolysis than for the HTL.

#### 4.4.2. Isobutanol

Cai et al. [30] studied WTW GHG emissions of isobutanol and found that a 72% reduction (25.9 g CO<sub>2</sub>-eq/MJ) in GHG emissions is possible to achieve compared to crude oil gasoline (93.3 g CO<sub>2</sub>-eq/MJ) [59]. However, this reduction requires a higher conversion of sugars to isobutanol, lower enzyme loading, and a shorter fermentation time. Moreover, Tao et al. [29] investigated the WTW GHG emissions of isobutanol. In their study, a 56% reduction in GHG emissions (41.2 g CO<sub>2</sub>-eq/MJ) could be obtained if the excess electricity was sold to the grid.

When assessing the production costs of isobutanol, the focus needs to be placed on genetically engineered microorganisms and integrated product removal. Consequently, feedstock cost becomes the largest concern, followed by capital costs. The available techno-economic assessment reached MFSP values of 1.90 €/L [27] and 1.24 €/L [30] for neat isobutanol. Cai et al. [30] obtained around 0.94 €/L as MFSP by increasing the yield of isobutanol, decreasing enzyme loading, and hydrolysis and fermentation times. Tao et al. [29] managed to obtain a lower MFSP of isobutanol, 0.81 €/L, for the fermentation process combined with continuous vacuum stripping.

#### 4.4.3. Experimentally Tested Fuel Blends

Figure 8 shows reductions in GHG emissions for the experimentally tested fuel blends. In this context, all oxygenated gasoline blends perform better than base gasoline. Due to the high energy content of renewable components, the largest GHG reductions could be obtained with the tested isobutanol blends: 21.7% and 21.5% for the isobutanol binary and ternary blends, respectively. In the calculations, the emission factor for neat anisole is 27.2 g CO<sub>2</sub>-eq/MJ [25], and for isobutanol, it is 25.9 g CO<sub>2</sub>-eq/MJ [30]. If the emission factor of anisole decreased to 20.5 g CO<sub>2</sub>-eq/MJ, according to the study by Cai et al. [30], the GHG reductions of anisole binary and ternary blends would be 11.7 and 22.5%, respectively. On the other hand, if the emission factor of isobutanol is increased to 41.2 g CO<sub>2</sub>-eq/MJ, according to the study by Tao et al. [29], the emission reductions for the isobutanol binary blend and ternary blend would be 16.8 and 19.0%, respectively.

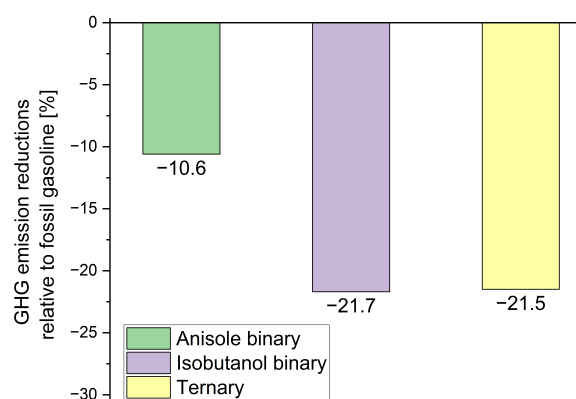


Figure 8. Reductions in well-to-wheel GHG emissions for experimentally tested fuel blends.

## 5. Conclusions

Anisole and isobutanol are very attractive SI fuel blending components, especially taking into account their potential to reduce GHG emissions if produced from lignocellulosic feedstock. From the end-use perspective, both chemical compounds have attractive

properties for SI engine applications, such as high RON, octane sensitivity, or an LHV close to that of gasoline. In conclusion, the proposed blends of anisole and isobutanol with base gasoline showed good potential as replacements for neat fossil gasoline. Engine tests enabled the validation of the formulated fuels in the intended environment. All tested fuels performed well in the SI engine and were recognized as drop-in solutions for a regular SI engine. The main conclusions of the study are the following:

- All selected blends performed well during experimental tests on the SI engine. No compatibility issues were detected, confirming the drop-in characteristic of all considered fuels. Fuels were stable and no phase separation was observed.
- In contrast to expectations, CO and HC emissions increased for oxygenated fuels, especially for alcohol blends. Nevertheless, the emissions of HC and CO and exhaust temperature were concluded to be in the range that can be accepted by TWC operation.
- Significantly higher BTE was observed for formulated blends when compared with base gasoline—on average, by 1.4%—which is in conformity with other studies.
- The potential of the anisole binary blend to decrease BSFC was reported. The estimated volumetric fuel consumption change (−1.8% for anisole binary, −1.4% for ternary and 4.6% in the case of the isobutanol binary blend) was better than expected based on LHV considerations.
- Tailpipe CO<sub>2</sub> emissions from engine tests were reduced on average by 5.1% for anisole binary and ternary blends and 7.9% for the isobutanol binary blend when compared to base gasoline.
- From a fleet perspective, modeled FC and CO<sub>2</sub> results were in line with experiments. An FFV with an optimized engine could benefit from the superior properties of anisole and isobutanol (high RON, oxygen content, heat of evaporation).
- The formulated blends can bring a decrease in GHG emissions, especially when looking at the WTW assessment. Significant reductions in GHG emissions were reported, ranging from 9.9 g CO<sub>2</sub>-eq/MJ for the anisole binary blend to 20.2 g CO<sub>2</sub>-eq/MJ for the isobutanol binary blend. These savings require sustainable lignocellulosic feedstock as well as advanced conversion processes such as hydrothermal liquefaction, fast pyrolysis, or fermentation.
- Further emission studies are needed to monitor particulates in exhaust gases from turbocharged direct injection SI engines. Additionally, extended compatibility studies are recommended, especially focusing on tests with elastomers.

**Author Contributions:** Conceptualization, M.W., M.d.P.B., R.T., A.K., A.S.-A. and M.L.; methodology, M.W., L.K., Y.K. and R.T.; software, Y.K., O.B. and M.W.; validation, O.B., J.K. and R.T.; formal analysis, M.W., L.K., Y.K. and J.K.; investigation, M.W., O.B., L.K., Y.K. and M.d.P.B.; resources, A.S.-A. and A.K.; data curation, M.W., L.K. and Y.K.; writing—original draft preparation, M.W., Y.K. and L.K.; writing—review and editing, M.W., J.K., L.K., Y.K., R.T., A.S.-A., M.d.P.B., M.L., A.K., O.B.; visualization, Y.K., M.W. and M.d.P.B.; supervision, M.L., A.S.-A., A.K. and R.T.; project administration, A.K. and A.S.-A.; funding acquisition, A.S.-A. and M.L. All authors have read and agreed to the published version of the manuscript.

**Funding:** This research was funded by Neste Corporation. The authors would like to also acknowledge support from Neste and Fortum Foundation, the branch group Combustion Engines Finland (Teknologiatoellisuus), Henry Ford Foundation and the Finnish Foundation for Technology Promotion (Tekniikan Edistämisseätiö).

**Institutional Review Board Statement:** Not applicable.

**Informed Consent Statement:** Not applicable.

**Acknowledgments:** The authors would like to thank Arpad Toldy and the “SI-Developers” team members (Katri Suistio, Julia Myllyviita, Tomi Juselius, and Sen Chen Xin) for their contribution to this work.

**Conflicts of Interest:** The authors declare no conflict of interest.

## Abbreviations

The following abbreviations are used in this manuscript:

BMEP	Brake mean effective pressure
BSFC	Brake specific fuel consumption
BTE	Brake thermal efficiency
CO	Carbon monoxide
CO <sub>2</sub>	Carbon dioxide
CO <sub>2</sub> -eq	Amount of carbon dioxide equivalent emissions
CR	Compression ratio
DI	Direct injection
E10	EN228 compliant gasoline with up to 10% ethanol vol. content
E85	High ethanol content gasoline for FFV
ECU	Engine control unit
EGR	Exhaust Gas Recirculation
EU	European Union
FC	Fuel consumption
FFV	Flexi-fuel vehicle
GHG	Greenhouse gases
HC	Unburned hydrocarbon emission
HTL	Hydro-thermal liquefaction
ICE	Internal combustion engine
LDV	Light-duty vehicle
LHV	Lower heating value
MFSP	Minimum fuel selling price
MON	Motor octane number
NECP	National Energy and Climate Plans
PFI	Port fuel injection
RED	Renewable Energy Directive
RON	Research octane number
rpm	Revolutions per minute
SI	Spark ignition
T50	Temperature at which 50% of the sample is evaporated
TWC	Three-way catalyst
wt.	Weight
WTW	Well-to-wheel
Greek letters	
$\alpha$	Volumetric fuel consumption
$\beta$	CO <sub>2</sub> emissions
$\rho$	Fuel density
Subscripts	
<i>mass</i>	On mass basis
<i>vol</i>	On volumetric basis
Symbols	
A	RON
B	Density
C	Carbon content
D	Volume-based LHV
H	Hydrogen content
O	Oxygen content
S	Sulfur content

## References

1. International Energy Agency. *Energy Technology Perspectives 2020*; International Energy Agency: Paris, France, 2020.
2. European Environment Agency. *Monitoring CO<sub>2</sub> Emissions from New Passenger Cars and Vans in 2018*; European Environment Agency: København, Denmark, 2020.
3. European Automobile Manufacturers Association. *Vehicles in Use—Europe 2019*; European Automobile Manufacturers Association: Brussels, Belgium, 2019.

4. European Environment Agency. *Transport: Increasing Oil Consumption and Greenhouse Gas Emissions Hamper EU Progress towards Environment and Climate Objectives*; European Environment Agency: København, Denmark, 2019.
5. Technology Collaboration Programme for International Energy Agency. *Advanced Motor Fuels Annual Report 2019*; Technology Collaboration Programme for International Energy Agency: Paris, France, 2019.
6. Eurostat. *Energy, Transport and Environment Statistics*, 2019th ed.; Eurostat: Luxembourg, 2019.
7. Regulation, E. *Regulation (EU) 2018/1999 of the European Parliament and of the Council of 11 December 2018 on the Governance of the Energy Union and Climate Action, amending Regulations (EC) No 663/2009 and (EC) No 715/2009 of the European Parliament and of the Council*; Technical Report, Directives 94/22/EC, 98/70/EC, 2009/31/EC, 2009/73/EC, 2010/31/EU, 2012/27; European Union: Brussels, Belgium 2018.
8. Ministry of Economic Affairs and Employment. *Finland's Integrated Energy and Climate Plan*; Ministry of Economic Affairs and Employment: Helsinki, Finland, 2019.
9. Finnish Ministry of Justice. *Act on the Promotion of the Use of Biofuels in Transport, Amendment 419/2019*; Finnish Ministry of Justice: Helsinki, Finland, 2019.
10. Red, I. *Directive (EU) 2018/2001 of the European Parliament and of the Council of 11 December 2018 on the Promotion of the Use of Energy from Renewable Source*; Publications Office of the European Union: Luxembourg, 2018.
11. International Energy Agency. *Global EV Outlook 2020: Entering the Decade of Electric Drive?* International Energy Agency: Paris, France, 2020.
12. European Automobile Manufacturers Association. *New Passenger Car Registrations by Fuel Type in the EU, Quarter 2*; European Automobile Manufacturers Association: Brussels, Belgium, 2020.
13. Berger, R. *Integrated Fuels and Vehicles Roadmap to 2030 and Beyond*; Roland Berger GmbH: Munich, Germany, 2016.
14. Van Dyk, S.; Su, J.; Mcmillan, J.D.; Saddler, J. Potential synergies of drop-in biofuel production with further co-processing at oil refineries. *Biofuels Bioprod. Biorefining* **2019**, *13*, 760–775. [[CrossRef](#)]
15. Engman, A.; Hartikka, T.; Honkanen, M.; Kiiski, U.; Kuronen, L.; Lehto, K.; Mikkonen, S.; Nortio, J.; Nuottimäki, J.; Saikkonen, P. *Neste Renewable Diesel Handbook*; Neste Proprietary Publication: Espoo, Finland, 2016.
16. Gaspar, D.J.; West, B.H.; Ruddy, D.; Wilke, T.J.; Polikarpov, E.; Alleman, T.L.; George, A.; Monroe, E.; Davis, R.W.; Vardon, D.; et al. *Top Ten Blendstocks Derived From Biomass For Turbocharged Spark Ignition Engines: Bio-Blendstocks with Potential for Highest Engine Efficiency*; Technical Report; Pacific Northwest National Lab.(PNNL): Richland, WA, USA, 2019.
17. Farrell, J.; Holladay, J.; Wagner, R. *Fuel Blendstocks with the Potential to Optimize Future Gasoline Engine Performance: Identification of Five Chemical Families for Detailed Evaluation*; US Department of Energy: Washington, DC, USA, 2018.
18. McCormick, R.L.; Fioroni, G.; Fouts, L.; Christensen, E.; Yanowitz, J.; Polikarpov, E.; Albrecht, K.; Gaspar, D.J.; Gladden, J.; George, A. Selection criteria and screening of potential biomass-derived streams as fuel blendstocks for advanced spark-ignition engines. *SAE Int. J. Fuels Lubr.* **2017**, *10*, 442–460. [[CrossRef](#)]
19. Miles, P. *Efficiency Merit Function for Spark-Ignition Engines: Revision and Improvements Based on FY16-17 Research*; US Department of Energy, Office of Energy Efficiency & Renewable Energy: Washington, DC, USA, 2018.
20. Szybist, J.P.; Busch, S.; McCormick, R.L.; Pihl, J.A.; Splitter, D.A.; Ratcliff, M.A.; Kolodziej, C.P.; Storey, J.M.; Moses-DeBusk, M.; Vuilleumier, D.; et al. What fuel properties enable higher thermal efficiency in spark-ignited engines? *Prog. Energy Combust. Sci.* **2021**, *82*, 100876. [[CrossRef](#)]
21. Ulonska, K.; König, A.; Klatt, M.; Mitsos, A.; Viell, J. Optimization of multiproduct biorefinery processes under consideration of biomass supply chain management and market developments. *Ind. Eng. Chem. Res.* **2018**, *57*, 6980–6991. [[CrossRef](#)]
22. Dahmen, M.; Marquardt, W. Model-based formulation of biofuel blends by simultaneous product and pathway design. *Energy Fuels* **2017**, *31*, 4096–4121. [[CrossRef](#)]
23. König, A.; Ulonska, K.; Mitsos, A.; Viell, J. Optimal applications and combinations of renewable fuel production from biomass and electricity. *Energy Fuels* **2019**, *33*, 1659–1672. [[CrossRef](#)]
24. König, A.; Neidhardt, L.; Viell, J.; Mitsos, A.; Dahmen, M. Integrated design of processes and products: Optimal renewable fuels. *Comput. Chem. Eng.* **2020**, *134*, 106712. [[CrossRef](#)]
25. Tews, I.J.; Zhu, Y.; Drennan, C.; Elliott, D.C.; Snowden-Swan, L.J.; Onarheim, K.; Solantausta, Y.; Beckman, D. Biomass Direct Liquefaction Options. In *TechnoEconomic and Life Cycle Assessment*; Technical Report; Pacific Northwest National Lab. (PNNL): Richland, WA, USA, 2014.
26. Rahzani, B.; Saidi, M.; Rahimpour, H.R.; Gates, B.C.; Rahimpour, M.R. Experimental investigation of upgrading of lignin-derived bio-oil component anisole catalyzed by carbon nanotube-supported molybdenum. *RSC Adv.* **2017**, *7*, 10545–10556. [[CrossRef](#)]
27. Roussos, A.; Misailidis, N.; Koulouris, A.; Zimbardi, F.; Petrides, D. A Feasibility Study of Cellulosic Isobutanol Production—Process Simulation and Economic Analysis. *Processes* **2019**, *7*, 667. [[CrossRef](#)]
28. Dunn, J.B.; Bidy, M.; Jones, S.; Cai, H.; Benavides, P.T.; Markham, J.; Tao, L.; Tan, E.; Kinchin, C.; Davis, R.; et al. Environmental, economic, and scalability considerations and trends of selected fuel economy-enhancing biomass-derived blendstocks. *ACS Sustain. Chem. Eng.* **2018**, *6*, 561–569. [[CrossRef](#)]
29. Tao, L.; Tan, E.C.; McCormick, R.; Zhang, M.; Aden, A.; He, X.; Zigler, B.T. Techno-economic analysis and life-cycle assessment of cellulosic isobutanol and comparison with cellulosic ethanol and n-butanol. *Biofuels Bioprod. Biorefining* **2014**, *8*, 30–48. [[CrossRef](#)]

30. Cai, H.; Markham, J.; Jones, S.; Benavides, P.T.; Dunn, J.B.; Bidy, M.; Tao, L.; Lamers, P.; Phillips, S. Techno-economic analysis and life-cycle analysis of two light-duty bioblendstocks: isobutanol and aromatic-rich hydrocarbons. *ACS Sustain. Chem. Eng.* **2018**, *6*, 8790–8800. [CrossRef]
31. Saidi, M.; Samimi, F.; Karimipourfard, D.; Nimmanwudipong, T.; Gates, B.C.; Rahimpour, M.R. Upgrading of lignin-derived bio-oils by catalytic hydrodeoxygenation. *Energy Environ. Sci.* **2014**, *7*, 103–129. [CrossRef]
32. Bi, Z.; Zhang, J.; Peterson, E.; Zhu, Z.; Xia, C.; Liang, Y.; Wiltowski, T. Biocrude from pretreated sorghum bagasse through catalytic hydrothermal liquefaction. *Fuel* **2017**, *188*, 112–120. [CrossRef]
33. Bridgwater, A.V. Review of fast pyrolysis of biomass and product upgrading. *Biomass Bioenergy* **2012**, *38*, 68–94. [CrossRef]
34. Laskar, D.D.; Yang, B.; Wang, H.; Lee, J. Pathways for biomass-derived lignin to hydrocarbon fuels. *Biofuels Bioprod. Biorefining* **2013**, *7*, 602–626. [CrossRef]
35. Ramirez, J.A.; Brown, R.J.; Rainey, T.J. A review of hydrothermal liquefaction bio-crude properties and prospects for upgrading to transportation fuels. *Energies* **2015**, *8*, 6765–6794. [CrossRef]
36. Christensen, E.; Fioroni, G.M.; Kim, S.; Fouts, L.; Gjersing, E.; Paton, R.S.; McCormick, R.L. Experimental and theoretical study of oxidative stability of alkylated furans used as gasoline blend components. *Fuel* **2018**, *212*, 576–585. [CrossRef]
37. Gschwend, D.; Soltic, P.; Wokaun, A.; Vogel, F. Review and performance evaluation of fifty alternative liquid fuels for spark-ignition engines. *Energy Fuels* **2019**, *33*, 2186–2196. [CrossRef]
38. Singerman, G.M. Novel Anisole Mixture and Gasoline Containing the Same. U.S. Patent 4,312,636, 26 January 1982.
39. Tian, M.; McCormick, R.L.; Ratcliff, M.A.; Luecke, J.; Yanowitz, J.; Glaude, P.A.; Cuijpers, M.; Boot, M.D. Performance of lignin derived compounds as octane boosters. *Fuel* **2017**, *189*, 284–292. [CrossRef]
40. Büttgen, R.; Tian, M.; Fenard, Y.; Minwegen, H.; Boot, M.; Heufer, K. An experimental, theoretical and kinetic modelling study on the reactivity of a lignin model compound anisole under engine-relevant conditions. *Fuel* **2020**, *269*, 117190. [CrossRef]
41. Wu, Y.; Rossow, B.; Modica, V.; Yu, X.; Wu, L.; Grisch, F. Laminar flame speed of lignocellulosic biomass-derived oxygenates and blends of gasoline/oxygenates. *Fuel* **2017**, *202*, 572–582. [CrossRef]
42. Szybist, J.P.; Splitter, D.A. Understanding chemistry-specific fuel differences at a constant RON in a boosted SI engine. *Fuel* **2018**, *217*, 370–381. [CrossRef]
43. Ratcliff, M.A.; Burton, J.; Sindler, P.; Christensen, E.; Fouts, L.; Chupka, G.M.; McCormick, R.L. Knock resistance and fine particle emissions for several biomass-derived oxygenates in a direct-injection spark-ignition engine. *SAE Int. J. Fuels Lubr.* **2016**, *9*, 59–70. [CrossRef]
44. da Silva Trindade, W.R.; dos Santos, R.G. Review on the characteristics of butanol, its production and use as fuel in internal combustion engines. *Renew. Sustain. Energy Rev.* **2017**, *69*, 642–651. [CrossRef]
45. Pugazhendhi, A.; Mathimani, T.; Varjani, S.; Rene, E.R.; Kumar, G.; Kim, S.H.; Ponnusamy, V.K.; Yoon, J.J. Biobutanol as a promising liquid fuel for the future—recent updates and perspectives. *Fuel* **2019**, *253*, 637–646. [CrossRef]
46. Al-Shorgani, N.K.N.; Shukor, H.; Abdeshahian, P.; Kalil, M.S.; Yusoff, W.M.W.; Hamid, A.A. Enhanced butanol production by optimization of medium parameters using *Clostridium acetobutylicum* YM1. *Saudi J. Biol. Sci.* **2018**, *25*, 1308–1321. [CrossRef]
47. Baez, A.; Cho, K.M.; Liao, J.C. High-flux isobutanol production using engineered *Escherichia coli*: a bioreactor study with in situ product removal. *Appl. Microbiol. Biotechnol.* **2011**, *90*, 1681–1690. [CrossRef]
48. Ryan, C. An Overview Of Gevo’s Biobased Isobutanol Production Process. *Gevo* **2021**. Available online: [https://www.google.com.hk/url?sa=t&rct=j&q=&esrc=s&source=web&cd=&ved=2ahUKewias82E\\_ZbyAhVDZc0KHTR3DYMqFnoECAQQAw&url=https%3A%2F%2Fgevo.com%2Fwp-content%2Fuploads%2F2019%2F11%2FGevo-WP\\_Isobutanol.1.pdf&usq=AOvVaw0jqSHDCstP-eO6YaU3-m0u](https://www.google.com.hk/url?sa=t&rct=j&q=&esrc=s&source=web&cd=&ved=2ahUKewias82E_ZbyAhVDZc0KHTR3DYMqFnoECAQQAw&url=https%3A%2F%2Fgevo.com%2Fwp-content%2Fuploads%2F2019%2F11%2FGevo-WP_Isobutanol.1.pdf&usq=AOvVaw0jqSHDCstP-eO6YaU3-m0u) (accessed on 8 May 2021).
49. Aakko-Saksa, P.; Koponen, P.; Kihlman, J.; Reinikainen, M.; Skyttä, E.; Rantanen-Kolehmainen, L.; Engman, A. *Biogasoline Options for Conventional Spark-Ignition Cars*; VTT Technical Research Centre of Finland: Espoo, Finland, 2011.
50. Irimescu, A. Fuel conversion efficiency of a port injection engine fueled with gasoline—Isobutanol blends. *Energy* **2011**, *36*, 3030–3035. [CrossRef]
51. Rodríguez-Antón, L.; Gutiérrez-Martín, F.; Hernández-Campos, M. Physical properties of gasoline-ETBE-isobutanol (in comparison with ethanol) ternary blends and their impact on regulatory compliance. *Energy* **2019**, *185*, 68–76. [CrossRef]
52. Stansfield, P.A.; Bisordi, A.; OudeNijeweme, D.; Williams, J.; Gold, M.; Ali, R. The Performance of a Modern Vehicle on a Variety of Alcohol-Gasoline Fuel Blends. *SAE Int. J. Fuels Lubr.* **2012**, *5*, 813–822. [CrossRef]
53. Karavalakis, G.; Short, D.; Vu, D.; Russell, R.; Asa-Awuku, A.; Durbin, T. A complete assessment of the emissions performance of ethanol blends and iso-butanol blends from a fleet of nine PFI and GDI vehicles. *SAE Int. J. Fuels Lubr.* **2015**, *8*, 374–395. [CrossRef]
54. Leone, T.G.; Anderson, J.E.; Davis, R.S.; Iqbal, A.; Reese, R.A.; Shelby, M.H.; Studzinski, W.M. The effect of compression ratio, fuel octane rating, and ethanol content on spark-ignition engine efficiency. *Environ. Sci. Technol.* **2015**, *49*, 10778–10789. [CrossRef]
55. Balki, M.K.; Sayin, C. The effect of compression ratio on the performance, emissions and combustion of an SI (spark ignition) engine fueled with pure ethanol, methanol and unleaded gasoline. *Energy* **2014**, *71*, 194–201. [CrossRef]
56. Akihisa, D.; Daisaku, S. *Research on Improving Thermal Efficiency Through Variable Super-High Expansion Ratio Cycle*; SAE Technical Report; SAE: Warrendale, PA, USA, 2010.
57. Curran, J.M. Air/Fuel Control System for Flexible Fuel Vehicles. U.S. Patent 5,253,631, 19 October 1993.

58. Deng, B.; Fu, J.; Zhang, D.; Yang, J.; Feng, R.; Liu, J.; Li, K.; Liu, X. The heat release analysis of bio-butanol/gasoline blends on a high speed SI (spark ignition) engine. *Energy* **2013**, *60*, 230–241. [[CrossRef](#)]
59. Edwards, R.; Padella, M.; Giuntoli, J.; Koeble, R.; O’Connell, A.; Bulgheroni, C.; Marelli, L. *Definition of Input Data to Assess GHG Default Emissions from Biofuels in EU Legislation*; Version 1c–July; Publications Office of the European Union: Luxembourg, 2017.
60. Robert Bosch GmbH. *Electronic Automotive Handbook*; Robert Bosch GmbH: Stuttgart, Germany, 2002; Volume 1.
61. Bielaczyc, P.; Woodburn, J.; Szczotka, A. Particulate emissions from European vehicles featuring direct injection spark ignition engines tested under laboratory conditions. *SAE Int. J. Fuels Lubr.* **2014**, *7*, 580–590. [[CrossRef](#)]
62. Kroyan, Y.; Wojcieszuk, M.; Kaario, O.; Larmi, M.; Zenger, K. Modeling the end-use performance of alternative fuels in light-duty vehicles. *Energy* **2020**, *205*, 117854. [[CrossRef](#)]
63. Anderson, J.; Kramer, U.; Mueller, S.; Wallington, T. Octane numbers of ethanol- and methanol- gasoline blends estimated from molar concentrations. *Energy Fuels* **2010**, *24*, 6576–6585. [[CrossRef](#)]
64. Wojcieszuk, M.; Kroyan, Y.; Larmi, M.; Kaario, O.; Bani, A. End-use performance of alternative fuels in various modes of transportation. *Adv. Proj. Deliv.* **2020**, *5*, 5.
65. Zabed, H.; Sahu, J.; Boyce, A.N.; Faruq, G. Fuel ethanol production from lignocellulosic biomass: an overview on feedstocks and technological approaches. *Renew. Sustain. Energy Rev.* **2016**, *66*, 751–774. [[CrossRef](#)]
66. Molino, A.; Chianese, S.; Musmarra, D. Biomass gasification technology: The state of the art overview. *J. Energy Chem.* **2016**, *25*, 10–25. [[CrossRef](#)]
67. Bagnato, G.; Sanna, A.; Paone, E.; Catizzone, E. Recent Catalytic Advances in Hydrotreatment Processes of Pyrolysis Bio-Oil. *Catalysts* **2021**, *11*, 157. [[CrossRef](#)]
68. Ahamed, T.S.; Anto, S.; Mathimani, T.; Brindhadevi, K.; Pugazhendhi, A. Upgrading of bio-oil from thermochemical conversion of various biomass—Mechanism, challenges and opportunities. *Fuel* **2020**, *287*, 119329. [[CrossRef](#)]
69. de Rezende Pinho, A.; de Almeida, M.B.; Mendes, F.L.; Casavechia, L.C.; Talmadge, M.S.; Kinchin, C.M.; Chum, H.L. Fast pyrolysis oil from pinewood chips co-processing with vacuum gas oil in an FCC unit for second generation fuel production. *Fuel* **2017**, *188*, 462–473. [[CrossRef](#)]
70. Castello, D.; Pedersen, T.H.; Rosendahl, L.A. Continuous hydrothermal liquefaction of biomass: A critical review. *Energies* **2018**, *11*, 3165. [[CrossRef](#)]
71. Funkenbusch, L.T.; Mullins, M.E.; Vamling, L.; Belkhiari, T.; Srettiwat, N.; Winjobi, O.; Shonnard, D.R.; Rogers, T.N. Technoeconomic assessment of hydrothermal liquefaction oil from lignin with catalytic upgrading for renewable fuel and chemical production. *Wiley Interdiscip. Rev. Energy Environ.* **2019**, *8*, e319. [[CrossRef](#)]
72. Funkenbusch, L.T.; Mullins, M.E.; Salam, M.A.; Creaser, D.; Olsson, L. Catalytic hydrotreatment of pyrolysis oil phenolic compounds over Pt/Al<sub>2</sub>O<sub>3</sub> and Pd/C. *Fuel* **2019**, *243*, 441–448. [[CrossRef](#)]
73. Wagnon, S.W.; Thion, S.; Nilsson, E.J.; Mehl, M.; Serinyel, Z.; Zhang, K.; Dagaut, P.; Konnov, A.A.; Dayma, G.; Pitz, W.J. Experimental and modeling studies of a biofuel surrogate compound: laminar burning velocities and jet-stirred reactor measurements of anisole. *Combust. Flame* **2018**, *189*, 325–336. [[CrossRef](#)]
74. Yakovlev, V.; Khromova, S.; Sherstyuk, O.; Dundich, V.; Ermakov, D.Y.; Novopashina, V.; Lebedev, M.Y.; Bulavchenko, O.; Parmon, V. Development of new catalytic systems for upgraded bio-fuels production from bio-crude-oil and biodiesel. *Catal. Today* **2009**, *144*, 362–366. [[CrossRef](#)]
75. Si, Z.; Zhang, X.; Wang, C.; Ma, L.; Dong, R. An overview on catalytic hydrodeoxygenation of pyrolysis oil and its model compounds. *Catalysts* **2017**, *7*, 169. [[CrossRef](#)]
76. Yang, Y.; Liu, X.; Xu, Y.; Gao, X.; Dai, Y.; Tang, Y. Palladium-Incorporated  $\alpha$ -MoC Mesoporous Composites for Enhanced Direct Hydrodeoxygenation of Anisole. *Catalysts* **2021**, *11*, 370. [[CrossRef](#)]
77. Taghvaei, H.; Kheirollahivash, M.; Ghasemi, M.; Rostami, P.; Gates, B.C.; Rahimpour, M.R. Upgrading of anisole in a dielectric barrier discharge plasma reactor. *Energy Fuels* **2014**, *28*, 4545–4553. [[CrossRef](#)]
78. Wang, H.; Feng, M.; Yang, B. Catalytic hydrodeoxygenation of anisole: an insight into the role of metals in transalkylation reactions in bio-oil upgrading. *Green Chem.* **2017**, *19*, 1668–1673. [[CrossRef](#)]
79. Talvenmaa, P. Introduction to chromic materials. In *Intelligent Textiles and Clothing*; Woodhead Publishing in Textiles: Cambridge, UK, 2006; pp. 193–205.
80. Durbin, T.D.; Karavalakis, G.; Norbeck, J.M.; Park, C.S.; Castillo, J.; Rheem, Y.; Bumiller, K.; Yang, J.; Van, V.; Hunter, K. Material compatibility evaluation for elastomers, plastics, and metals exposed to ethanol and butanol blends. *Fuel* **2016**, *163*, 248–259. [[CrossRef](#)]
81. McCormick, R.L.; Ratcliff, M.A.; Christensen, E.; Fouts, L.; Luecke, J.; Chupka, G.M.; Yanowitz, J.; Tian, M.; Boot, M. Properties of oxygenates found in upgraded biomass pyrolysis oil as components of spark and compression ignition engine fuels. *Energy Fuels* **2015**, *29*, 2453–2461. [[CrossRef](#)]
82. Vom Lehn, F.; Cai, L.; Tripathi, R.; Broda, R.; Pitsch, H. A property database of fuel compounds with emphasis on spark-ignition engine applications. *Appl. Energy Combust. Sci.* **2021**, *5*, 100018.
83. Zervas, E.; Montagne, X.; Lahaye, J. Emissions of regulated pollutants from a spark ignition engine. Influence of fuel and air/fuel equivalence ratio. *Environ. Sci. Technol.* **2003**, *37*, 3232–3238. [[CrossRef](#)]
84. Elfassakhany, A. State of art of using biofuels in spark ignition engines. *Energies* **2021**, *14*, 779. [[CrossRef](#)]

85. Larsson, T.; Mahendar, S.K.; Christiansen-Erlandsson, A.; Olofsson, U. The Effect of Pure Oxygenated Biofuels on Efficiency and Emissions in a Gasoline Optimised DISI Engine. *Energies* **2021**, *14*, 3908. [[CrossRef](#)]
86. Yusoff, M.; Zulkifli, N.; Masum, B.; Masjuki, H. Feasibility of bioethanol and biobutanol as transportation fuel in spark-ignition engine: A review. *RSC Adv.* **2015**, *5*, 100184–100211. [[CrossRef](#)]
87. Gökteş, M.; Balki, M.K.; Sayin, C.; Canakci, M. An evaluation of the use of alcohol fuels in SI engines in terms of performance, emission and combustion characteristics: A review. *Fuel* **2021**, *286*, 119425. [[CrossRef](#)]
88. Elfasakhany, A. Dual and Ternary Biofuel Blends for Desalination Process: Emissions and Heat Recovered Assessment. *Energies* **2021**, *14*, 61. [[CrossRef](#)]
89. Bielaczyc, P.; Woodburn, J.; Klimkiewicz, D.; Pajdowski, P.; Szczotka, A. An examination of the effect of ethanol–gasoline blends' physicochemical properties on emissions from a light-duty spark ignition engine. *Fuel Process. Technol.* **2013**, *107*, 50–63. [[CrossRef](#)]
90. Regalbutto, C.; Pennisi, M.; Wigg, B.; Kyritsis, D. *Experimental Investigation of Butanol Isomer Combustion in Spark Ignition Engines*; SAE Technical Report; SAE: Warrendale, PA, USA, 2012.
91. Nithyanandan, K.; Lee, C.F.F.; Wu, H.; Zhang, J. Performance and emissions of acetone-butanol-ethanol (ABE) and gasoline blends in a port fuel injected spark ignition engine. In *Internal Combustion Engine Division Fall Technical Conference*; American Society of Mechanical Engineers: New York, NY, USA, 2014; Volume 46162, p. V001T02A010.
92. Dernote, J.; Mounaïm-Rousselle, C.; Halter, F.; Seers, P. Evaluation of butanol–gasoline blends in a port fuel-injection, spark-ignition engine. *Oil Gas Sci. Technol. Rev. L'Institut Français Pétrole* **2010**, *65*, 345–351. [[CrossRef](#)]
93. Masum, B.; Kalam, M.; Masjuki, H.; Palash, S.; Fattah, I.R. Performance and emission analysis of a multi cylinder gasoline engine operating at different alcohol–Gasoline blends. *RSC Adv.* **2014**, *4*, 27898–27904. [[CrossRef](#)]
94. Sayin, C. The impact of varying spark timing at different octane numbers on the performance and emission characteristics in a gasoline engine. *Fuel* **2012**, *97*, 856–861. [[CrossRef](#)]
95. Sayin, C.; Balki, M.K. Effect of compression ratio on the emission, performance and combustion characteristics of a gasoline engine fueled with iso-butanol/gasoline blends. *Energy* **2015**, *82*, 550–555. [[CrossRef](#)]
96. Laurikko, J. *On Exhaust Emissions from Petrol-Fuelled Passenger Cars at Low Ambient Temperatures*; Technical Research Centre of Finland: Espoo, Finland, 1998.
97. Meyer, P.A.; Snowden-Swan, L.J.; Jones, S.B.; Rappé, K.G.; Hartley, D.S. The effect of feedstock composition on fast pyrolysis and upgrading to transportation fuels: Techno-economic analysis and greenhouse gas life cycle analysis. *Fuel* **2020**, *259*, 116218. [[CrossRef](#)]
98. Nie, Y.; Bi, X. Life-cycle assessment of transportation biofuels from hydrothermal liquefaction of forest residues in British Columbia. *Biotechnol. Biofuels* **2018**, *11*, 23. [[CrossRef](#)]
99. Zhu, Y.; Bidy, M.J.; Jones, S.B.; Elliott, D.C.; Schmidt, A.J. Techno-economic analysis of liquid fuel production from woody biomass via hydrothermal liquefaction (HTL) and upgrading. *Appl. Energy* **2014**, *129*, 384–394. [[CrossRef](#)]